



# Southern Ocean phytoplankton under climate change: shifting balance of bottom-up and top-down control

Tianfei Xue<sup>1</sup>, Ivy Frenger<sup>1</sup>, Jens Terhaar<sup>2</sup>, A.E. Friederike Prowe<sup>1</sup>, Thomas L. Frölicher<sup>3,4</sup>, and Andreas Oschlies<sup>1</sup>

<sup>1</sup>GEOMAR Helmholtz Centre for Ocean Research Kiel, Kiel, Germany

<sup>2</sup>Department of Marine Chemistry and Geochemistry, Woods Hole Oceanographic Institution, Woods Hole, Massachusetts, USA

<sup>3</sup>Climate and Environmental Physics, Physics Institute, University of Bern, Bern, Switzerland

<sup>4</sup>Oeschger Centre for Climate Change Research, University of Bern, Bern, Switzerland

**Correspondence:** Tianfei Xue (txue@geomar.de)

**Abstract.** Phytoplankton forms the base of the marine food web by transforming CO<sub>2</sub> into organic carbon via photosynthesis. Some of the organic carbon is then transferred through the food web and exported into the deep ocean, a process known as the biological carbon pump. Despite the importance of phytoplankton for marine ecosystems and the global carbon cycle, projections of phytoplankton biomass in response to climate change differ strongly across Earth system models, illustrating uncertainty in our understanding of the underlying processes. Differences are especially large in the Southern Ocean, a region that is notoriously difficult to represent in models. Here, we argue that water column-integrated phytoplankton biomass in the Southern Ocean is projected to largely remain unchanged under climate change by the CMIP6 multi-model ensemble because of a shifting balance of bottom-up and top-down processes driven by a shoaling mixed layer depth. A shallower mixed layer is projected to improve growth conditions and consequently weaken bottom-up control. In addition to enhanced phytoplankton growth, the shoaling of the mixed layer also compresses phytoplankton closer to the surface and promotes zooplankton grazing efficiency, thus intensifying top-down control. Overall, our results suggest that while changes in bottom-up conditions stimulate enhanced growth, intensified top-down control opposes an increase in phytoplankton and becomes increasingly important for phytoplankton response under climate change in the Southern Ocean.

## 1 Introduction

Phytoplankton is fundamental to the marine ecosystem and the global carbon cycle, as it is the base of the ocean food web (Pauly and Christensen, 1995) and accounts for approximately half of the global biological carbon fixation (Field et al., 1998). Despite the importance of phytoplankton for future changes in the ecosystem and carbon cycle, its response to climate change remains uncertain. Earth system model projections of phytoplankton biomass and its growth for the 21<sup>st</sup> century reveal large uncertainties (Steinacher et al., 2010; Laufkötter et al., 2015; Frölicher et al., 2016; Tagliabue et al., 2021) and even the direction of changes remains unclear (Bopp et al., 2022). The uncertainties are due not only to uncertainties in the underlying physical forcing but also to different biological and biogeochemical parameterizations of processes in the models (Laufkötter et al.,



2015). Such uncertainties have the potential to propagate through the food web, often amplified by poorly simulated food web dynamics (Stock et al., 2014b), and cause even greater uncertainties for higher trophic level projections (Lotze et al., 2019). In turn, uncertainties in higher trophic level projections and poorly simulated food web dynamics will, through ill-constrained grazing pressure on phytoplankton, lead to amplified uncertainties in phytoplankton projections, forming a feedback loop for uncertainties in simulated ecosystem dynamics. Given the role of phytoplankton in marine ecosystems and biogeochemical cycling, better constraining how phytoplankton respond to changes in their physical, chemical and biological environment under climate change is critical.

Climate change affects phytoplankton through both "bottom-up" (Marinov et al., 2010; Leung et al., 2015) and "top-down" (Stock et al., 2014a; Kwiatkowski et al., 2019) control. Bottom-up control describes changes of phytoplankton growth due to changes in light, temperature, and nutrients caused by environmental factors like mixing or upwelling (Behrenfeld et al., 2006). Given that these environmental factors are projected to change under climate change, phytoplankton will also be influenced by climate change. Top-down control, on the other hand, describes how phytoplankton responds to predator changes. The major predator of phytoplankton is zooplankton. Changes in phytoplankton are typically described as top-down controlled if changes in zooplankton and phytoplankton are of the opposite sign (Chust et al., 2014), for example, when phytoplankton decreases while zooplankton increases. Globally, changes in bottom-up control are thought to dominate the phytoplankton response to changing climate, with a decrease in phytoplankton biomass and growth due to reduced nutrient supply as a result of increasing ocean stratification and shoaling mixed layers (Sarmiento et al., 2004b; Bopp et al., 2005; Behrenfeld et al., 2006; Steinacher et al., 2010; Boyce et al., 2010). An opposite bottom-up response can be found in high-latitude regions where improved light conditions due to increased stratification are projected to lead to phytoplankton increases (Sarmiento et al., 2004b). Although predators and grazing pressure also evolve with climate change (Shurin et al., 2012), top-down control has received much less attention (Ratnarajah et al., 2023).

The Southern Ocean is a region where models, albeit with an uncertain magnitude, robustly project that phytoplankton will grow better with shoaling mixed layer depths under global warming (Fig. 1 & 2; Sarmiento et al., 2004b; Bopp et al., 2013; Laufkötter et al., 2015; Kwiatkowski et al., 2020). Despite the high abundance of macronutrients (Fig. A1), phytoplankton growth in the Southern Ocean is at present largely bottom-up controlled by iron and light limitations (Martin et al., 1990; Mitchell et al., 1991; Arteaga et al., 2020; Moore et al., 2013). Light limitation is especially strong in the Southern Ocean due to the deep mixed layers and low surface radiation in mid-to-high latitude winters. Under global warming, Southern Ocean phytoplankton growth conditions are anticipated to improve with rising temperatures and a prolonged growing season, as well as improving light conditions with increasing stratification and shoaling mixed layer depths (Bopp et al., 2001; Sarmiento et al., 2004b). Apart from the prominent limitation by light, changes in phytoplankton iron limitation with climate change remain uncertain as the iron cycle is not well resolved mechanistically in current Earth System Models (Tagliabue et al., 2016). In addition to bottom-up control, top-down control via zooplankton also affects phytoplankton variability in the Southern Ocean (Le Quéré et al., 2016). As phytoplankton in the Southern Ocean plays an important role in setting the biogeochemical characteristics of ocean waters globally, better understanding and constraining its evolution under climate change is relevant



for reliable projections of marine biological production well beyond the Southern Ocean (Sarmiento et al., 2004a; Marinov et al., 2006; Nissen et al., 2021).

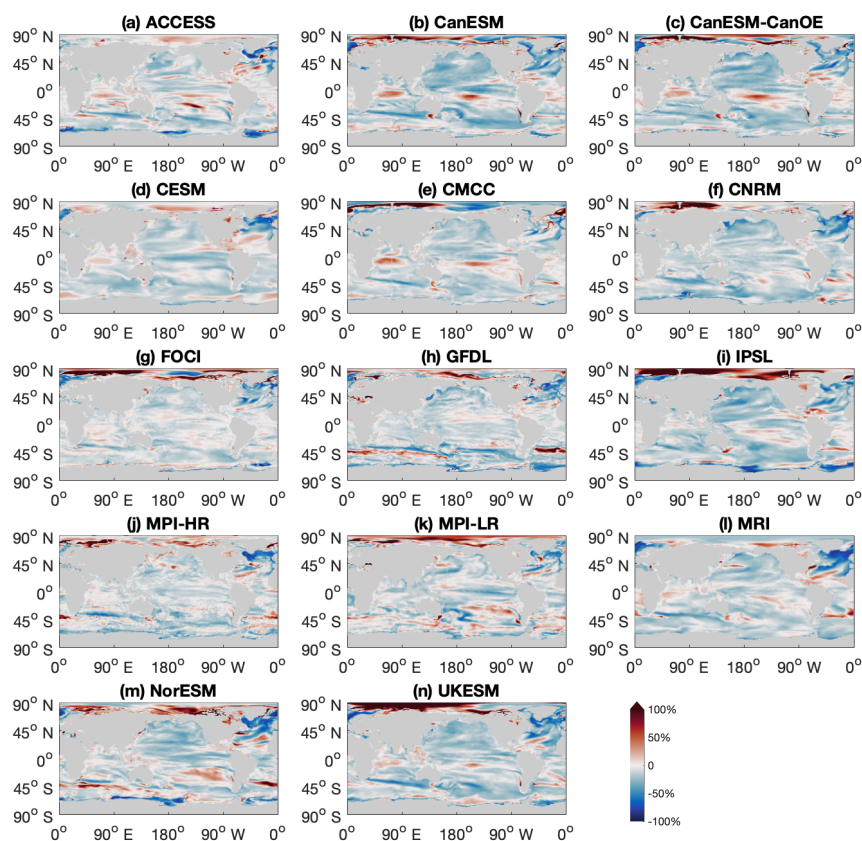


**Figure 1.** Maps for individual climate models, showing annual mean mixed layer depth anomalies of the last decade (2090s) of the 21<sup>st</sup> century relative to the first decade (2000s), under a high emissions, no mitigation scenario (SSP5-8.5). Red indicates deepening, and blue indicates shoaling mixed layers. Results are shown for a multi-model ensemble (MME; listed in Table 1).

## 2 Methods

### 2.1 Research area

60 This study focuses on the subantarctic and subpolar Antarctic regions, which approximately span the latitude range of 40°S–60°S. This region has sufficiently high macronutrient levels to support the growth of phytoplankton and is relatively little affected by the sea ice. Earth System Models project that surface chlorophyll levels in this region will increase with global warming (Fig. 3). Under the current climate, the observed seasonal cycle of surface phytoplankton in the subantarctic and subpolar

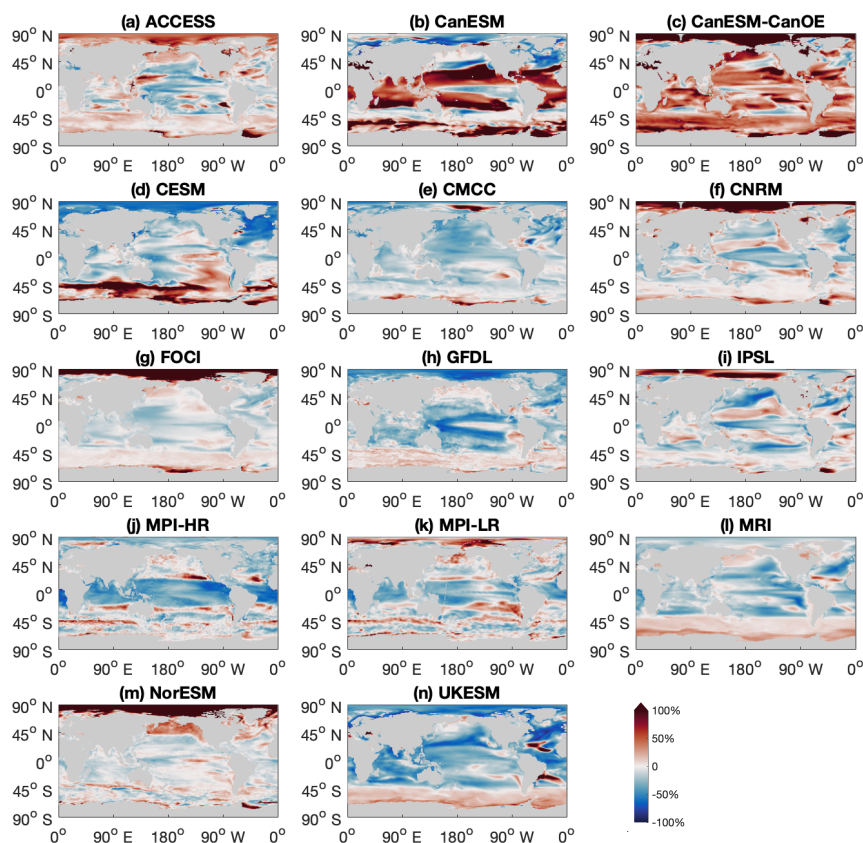


**Figure 2.** Maps for individual climate models, showing the relative variation of surface chlorophyll of the last decade (2090s) of the 21<sup>st</sup> century relative to the first decade (2000s), under a high emissions, no mitigation scenario (SSP5-8.5). Red indicates increasing and blue indicates decreasing surface chlorophyll during the 21<sup>st</sup> century. Results are shown for a multi-model ensemble (MME; listed in Table 1).

Antarctic regions is found to be strongly driven by the light limitation due to the seasonal change in mixed layer depth (MLD; Arteaga et al., 2020).

## 2.2 Multi-Model Ensemble

Here we use the output of a Multi-Model Ensemble (MME; Table 1) of 14 Earth System Models (ESMs). Of the 14 models that we used, 13 ESMs are part of the Coupled Model Intercomparison Project Phase 6 (CMIP6, downloaded from <https://esgf-data.dkrz.de>). The FOCI (Flexible Ocean and Climate Infrastructure) model run at GEOMAR (Chien et al., 2022) was added to these 13 models. The selection of these models is based on the present availability of the variables required (phytoplankton biomass concentration, zooplankton biomass concentration, mixed layer depth and surface chlorophyll concentration), the temporal resolution (monthly), and the experimental settings (historical simulation, piControl simulation to account for potential drifts, and the SSP5-8.5 high emission no mitigation scenario). The models within the MME are structurally different, cover a range

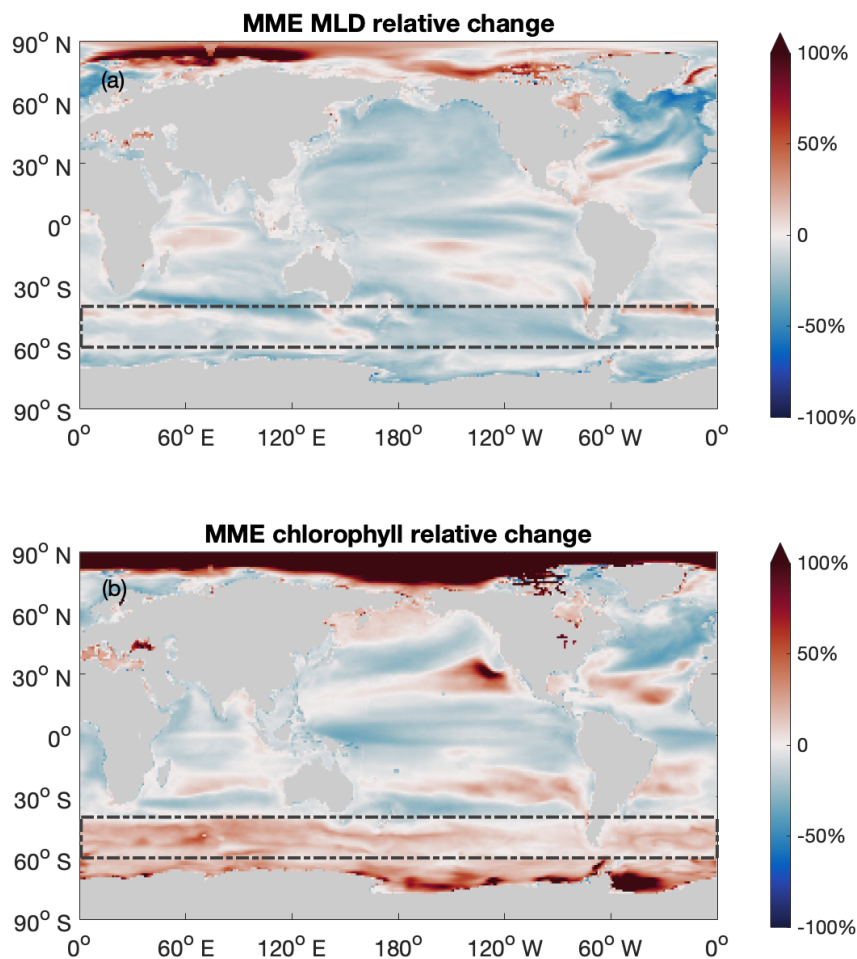


**Figure 3.** The Southern Ocean stands out as a region with projected shoaling mixed layers and increasing chlorophyll under a high emission, no mitigation scenario (SSP5-8.5). Global maps of relative change in (a) mixed layer depth (MLD) and (b) surface chlorophyll with global warming (between the first (2000s) and last decade (2090s) of the 21<sup>st</sup> century). Black boxes mark the focus area. Red indicates deepening mixed layers and increasing surface chlorophyll, while blue indicates shoaling mixed layers and decreasing surface chlorophyll towards the end of the 21<sup>st</sup> century. Results are shown for a multi-model ensemble (MME; listed in Table 1).



**Table 1.** Overview of the Multi-Model Ensemble (MME) used in this study.

Number	Model Name	Ocean	Plankton	Simulations		Reference
		Biogeochemistry	Groups	biomass	production	
(a)	ACCESS-ESM1-5	WOMBAT*	P1Z1	(✓)		Ziehn et al. (2020)
(b)	CanESM5	CMOC	P1Z1	✓		Swart et al. (2019)
(c)	CanESM5-CanOE	CanOE*	P2Z2	✓	✓	Christian et al. (2022)
(d)	CESM2-WACCM	MARBL*	P3Z1	✓		Danabasoglu et al. (2020)
(e)	CMCC-ESM2	BFM v5.2*	P2Z2	(✓)		Lovato et al. (2022)
(f)	CNRM-ESM2-1	PISCESv2-gas*	P2Z2	✓	✓	Séférian et al. (2019)
(g)	FOCI1	MOPS	P1Z1	✓	✓	Chien et al. (2022)
(h)	GFDL-ESM4	COBALTv2*	P3Z3	✓	✓	Dunne et al. (2020)
(i)	IPSL-CM6A-LR	PISCES-v2*	P2Z2	✓		Boucher et al. (2020)
(j)	MPI-ESM1.2-HR	HAMOCC6*	P2Z1	✓	✓	Müller et al. (2018)
(k)	MPI-ESM1.2-LR	HAMOCC6 *	P2Z1	✓	✓	Mauritsen et al. (2019)
(l)	MRI-ESM2.0	NPZD	P1Z1	✓		Tsujino et al. (2017)
(m)	NorESM2-MM	iHAMOCC*	P2Z1	✓		Tjiputra et al. (2020)
(n)	UKESM1-0-LL	MEDUSA *	P2Z2	✓	✓	Sellar et al. (2019)

\* indicates models that explicitly include iron limitation.

PxZy in column "Plankton Groups" indicates x phytoplankton and y zooplankton groups in the respective model.

Column "Simulations" indicates models whose output was used in biomass or production relevant calculations.

(✓) indicates models that do not provide phytoplankton and zooplankton biomass as output but chlorophyll concentration, therefore they are used only to constrain the change of phytoplankton concentration based on chlorophyll in section 3.3.2

of different parameterizations of processes, and initial conditions (Séférian et al., 2020). All output fields were regridded on a  
 75 regular  $1^\circ \times 1^\circ$  map using the bilinear interpolation of CDO (Climate Data Operators).

### 2.3 Emergent constraint

The emergent constraint approach is based on an identifiable relationship in a model ensemble between an observable contemporary sensitivity and an uncertain condition for future climates (Hall et al., 2019; Williamson et al., 2021). The observable contemporary condition can then be used to constrain future model projections (such as previously done for tropical marine primary productivity in Kwiatkowski et al. (2017), ocean carbon sink in Kessler and Tjiputra (2016); Terhaar et al. (2021a, 2022), and ocean acidification in Terhaar et al. (2020, 2021b)).

Here, we apply the emergent constraint approach to reduce uncertainties of the projections of the long-term sensitivity of chlorophyll to changes in the mixed layer depth ( $S_{clm}$ , Eq. 2, period: 2000 - 2099) using contemporary seasonal sensitivities of chlorophyll to mixed layer depth changes ( $S_{seas}$ , Eq. 1, period: 2000 - 2009). For each of the individual models and for the  
 85 observations, the respective contemporary seasonal sensitivity of chlorophyll to the MLD ( $S_{seas}$ ) is computed as follows:

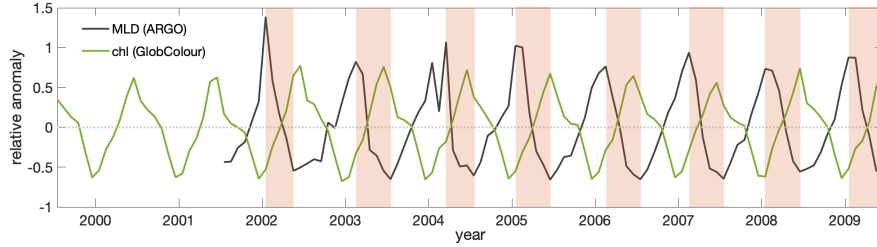


**Figure 4.** The surface chlorophyll (chl) concentration shows a clear seasonal cycle that is anticorrelated with mixed layer depths (MLD) in observations. Contemporary seasonal variations relative to the respective annual means of observed MLD (ARGO: black) and surface chlorophyll concentration based on merged satellite data (GlobColour: green) in the Southern Ocean subantarctic and subpolar Antarctic regions (40°S–60°S). The shaded areas indicate the seasonal MLD shoaling period.

$$S_{seas} = \frac{(\overline{chl_{mmax}} - \overline{chl_{mmin}}) / \overline{chl}}{(\overline{MLD_{mmax}} - \overline{MLD_{mmin}}) / \overline{MLD}}, \quad (1)$$

with overlines indicating the annual mean and *mmax* and *mmin* indicating the months with the minimum and maximum MLD that mark the beginning and the end of the shoaling period (shaded periods in Fig. 4). We explicitly selected the shoaling period, as the decrease due to MLD shoaling and improving light conditions are analogues to changes under climate change.

90 Following the definition of the seasonal sensitivity in Eq. 1, the long-term sensitivities ( $S_{clm}$ , Eq. 2) of individual models are calculated based on the differences between the first (2000s) and last (2090s) decade of the 21<sup>st</sup> century in chlorophyll ( $R_{chl}$ ) and MLD ( $R_{MLD}$ ), each normalised with respect to the first decade of the century.

$$S_{clm} = \frac{(\overline{chl_{2090s}} - \overline{chl_{2000s}}) / \overline{chl_{2000s}}}{(\overline{MLD_{2090s}} - \overline{MLD_{2000s}}) / \overline{MLD_{2000s}}} = \frac{R_{chl}}{R_{MLD}} \quad (2)$$

95 Relative MLD anomalies are used instead of absolute anomalies, as the relative anomaly relates to the dilution of phytoplankton across the mixed layer, which is one of the main mechanisms controlling the surface phytoplankton concentration. Despite the large differences revealed in the absolute MLD and chlorophyll values of individual models (Fig. A2), the models resolve the same anticorrelation between relative variations of MLD and chlorophyll as seen in observations (Fig. 9).

100 The probability density functions (PDFs) of the long-term sensitivity ( $S_{clm}$ ) were derived from a Gaussian distribution and the MME mean and standard deviation, assuming that all models have equal probability (Fig. 10b). We calculated the constrained PDFs following previous literature (Eq. 3; Eq. 20 in Williamson et al., 2021).

$$p(y) = \int_{-\infty}^{\infty} p(y | x) p(x) dx = \mathcal{N} \left( y \mid a + bX_{obs}, \sqrt{\sigma_f^2 + b^2\sigma_{obs}^2} \right) \quad (3)$$



The mean of the distribution is calculated by applying the observational constraint ( $X_{obs}$ ) to the emergent linear inter-model relationship ( $y = a + b * x$ ) of  $S_{seas}$  and  $S_{clm}$ . The standard deviation of the PDF distribution is estimated by accounting for both observational uncertainty ( $\sigma_{obs}$ ) and the prediction interval of the emergent relationship ( $\sigma_f$ ).

105 The constrained  $S_{clm}$  (here defined as  $S_{clm^*}$ ) is then used to estimate the constrained surface chlorophyll change by the end of the 21<sup>st</sup> century ( $R_{clm^*}$ ) by reordering Eq. 2 to  $R_{clm^*} = R_{MLD} * S_{clm^*}$ . The uncertainty in the post-constraint projection for the relative variation of chlorophyll is then calculated by accounting for uncertainties from both the estimation of the constrained long-term sensitivity ( $\sigma_{S_{clm^*}}$ ) and the MLD projection ( $\sigma_{R_{MLD}}$ ) through error propagation:

$$\mathcal{N}(R_{chl^*}, \sigma_{chl^*}) = \mathcal{N}\left(R_{MLD} \cdot S_{clm^*}, |R_{MLD} \cdot S_{clm^*}| \sqrt{\left(\frac{\sigma_{R_{MLD}}}{R_{MLD}}\right)^2 + \left(\frac{\sigma_{S_{clm^*}}}{S_{clm^*}}\right)^2}\right) \quad (4)$$

## 110 2.4 Observational constraints

The observation-based estimate of  $S_{seas}$  is based on monthly MLD data from the ARGO mixed layer database (<http://mixedlayer.ucsd.edu/>) and satellite-derived monthly surface chlorophyll data from the merged satellite product GlobColour (<https://www.globcolour.info/>) during the period 2000 - 2009. The observational MLD is calculated based on the temperature threshold estimate (threshold of 0.2°C; Holte and Talley, 2009), consistent with the MLD diagnostic available from the MME.

115 Surface chlorophyll is used as a proxy for surface phytoplankton concentration (Fig. A3). It is a comparatively well-observed variable, in contrast to phytoplankton biomass. The seasonal variation in the observability of the satellite surface chlorophyll data is mainly affected by the winter light conditions and varying ice cover to the south of the research region. The impact of cloud cover in the research region is minor at a monthly temporal resolution (Fig. A4).

## 2.5 Trophic transfer efficiency

120 The trophic transfer efficiency (TTE, Eq. 5) is defined as the ratio of depth-integrated biomass of zooplankton to depth-integrated biomass of phytoplankton following Barnes et al. (2010),

$$TTE = \frac{\sum_{z=0}^{zmax} zoo * dh}{\sum_{z=0}^{zmax} phy * dh} \quad (5)$$

where phy and zoo represent the phytoplankton and zooplankton biomass concentrations (unit:  $mg C m^{-3}$ ), respectively; h indicates the thickness of each grid box, and zmax the depth of the water column.

125 The dimensionless TTE reflects the biomass or energy transfer between trophic levels and is typically estimated based on the biomasses or productivities of trophic levels. We used biomass instead of productivity to quantify the TTE, as biomass can be directly compared to observations and is available from more models than productivity data (Table 1).





### 3 Results

#### 3.1 Stable phytoplankton biomass in a changing climate: shifting balance of bottom-up and top-down control in the Southern Ocean

130

The multi-model ensemble (MME) projects the depth-integrated phytoplankton biomass to remain relatively stable ( $-1 \pm 7\%$ ) throughout the 21<sup>st</sup> century following the SSP5-8.5 scenario (Fig. 5a). Across the ensemble of Earth system models, individual projections range from -10% to 15% in the 2090s compared to the 2000s. Future trends in depth-integrated phytoplankton biomass are determined by the competing effects of increasing primary production (bottom-up, Fig. 5b) and grazing by zoo-  
135 plankton (top-down, Fig. 5c). Understanding the complex interplay between bottom-up and top-down controls is crucial for projecting how phytoplankton will respond to future climate change.

Projected increases in primary production ( $10 \pm 11\%$ ) show that phytoplankton growth conditions are improving with climate change, indicating weakening bottom-up control (Fig. 5b). On these centennial timescales, climate change-induced changes in primary production in the subantarctic and subpolar Antarctic regions are tightly coupled to MLD-driven bottom-  
140 up changes (e.g., light, nutrients) that also drive changes on seasonal timescales (Arteaga et al., 2020; Leung et al., 2015). As the MLD is projected to shoal by  $12 \pm 5\%$  over the course of the 21<sup>st</sup> century (Fig. 6a), phytoplankton in the water column will not be passively mixed down, stay closer to the surface, and experience better light conditions. As a result, phytoplankton is projected to have a higher growth rate (dashed line in Fig. 5b).

Despite increasing primary production, the phytoplankton biomass remains stable throughout the 21<sup>st</sup> century because of  
145 enhanced zooplankton grazing ( $14 \pm 15\%$ ), thus intensified top-down control (Fig. 5c). With top-down control exhibiting a similar increasing trend as bottom-up condition under climate change, phytoplankton biomass stays in a dynamic balance despite the flux changes, and thereby appears not to respond to the changing climate. An enhanced role of grazing under climate change is consistent with findings in Laufkötter et al. (2015).

#### 3.2 Increasing phytoplankton concentration: intensified top-down control shifts trophic structure

150 The increasing top-down control and grazing pressure on phytoplankton is a consequence of rising phytoplankton concentrations under climate change due to mixed layer shoaling (Fig. 6b). Apart from total phytoplankton biomass, which reflects the total amount of food available to zooplankton, the concentration of phytoplankton is also a crucial factor in zooplankton grazing. The feeding efficiency of zooplankton depends directly on the concentration of phytoplankton. When phytoplankton concentration increases with shoaling mixed layer depths, it leads to a higher encounter efficiency between zooplankton (the  
155 predator) and phytoplankton (the prey), which enables zooplankton to graze more efficiently. A shoaling mixed layer enhances phytoplankton concentration and supports a higher grazing efficiency for zooplankton, which in turn results in greater grazing pressure on phytoplankton (dashed line in Fig. 5c) and thus leads to a stronger top-down control on phytoplankton. This mechanism is apparent in the significant correlation between mixed layer depth and phytoplankton grazing loss due to zooplankton on the long-term time scale (Fig. 7), and has previously been suggested to be important on a seasonal scale in present-day produc-  
160 tive systems (Xue et al., 2022a). While bottom-up growth conditions are improved (in a nutrient-replenished upwelling system

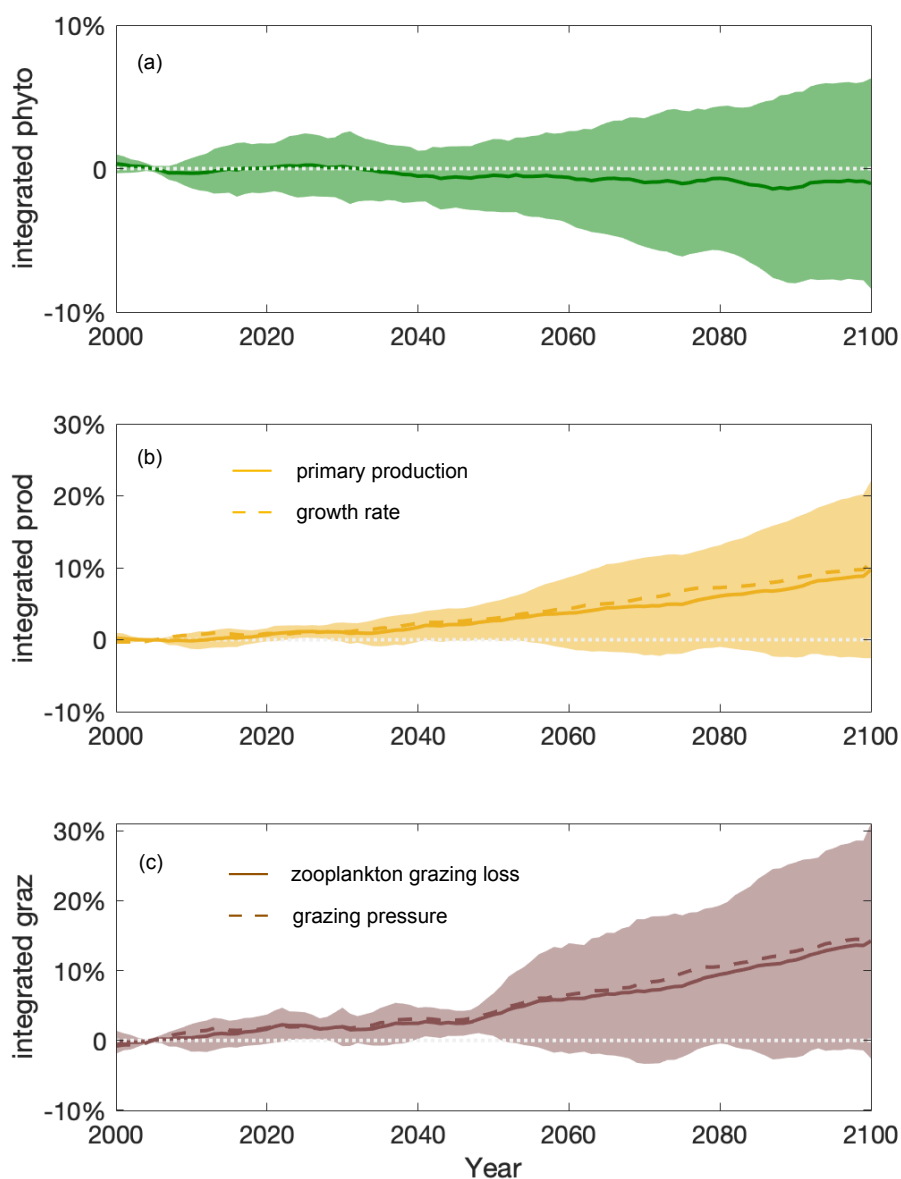


**Figure 5. Stable integrated phytoplankton projections over the course of the 21<sup>st</sup> century due to a shifting balance of bottom-up and top-down control.** Multi-model ensemble (MME) projections of the relative changes of depth-integrated (a) phytoplankton (phyto, dark green), (b) phytoplankton production (prod, yellow) and (c) grazing loss from zooplankton (graz, brown) from 2000 - 2100 under the SSP5-8.5 scenario, with shading indicating one standard deviation across the ESMs, relative to the respective mean values of the first decade of the 21<sup>st</sup> century (2000 - 2009) in the Southern Ocean. Solid lines indicate the multi-model mean. Dashed lines in (b) and (c) indicate the MME averaged phytoplankton growth rate (estimated as integrated production divided by integrated biomass) and grazing pressure (estimated as integrated grazing loss divided by integrated biomass), respectively. The time series are filtered using a 10-year moving average.

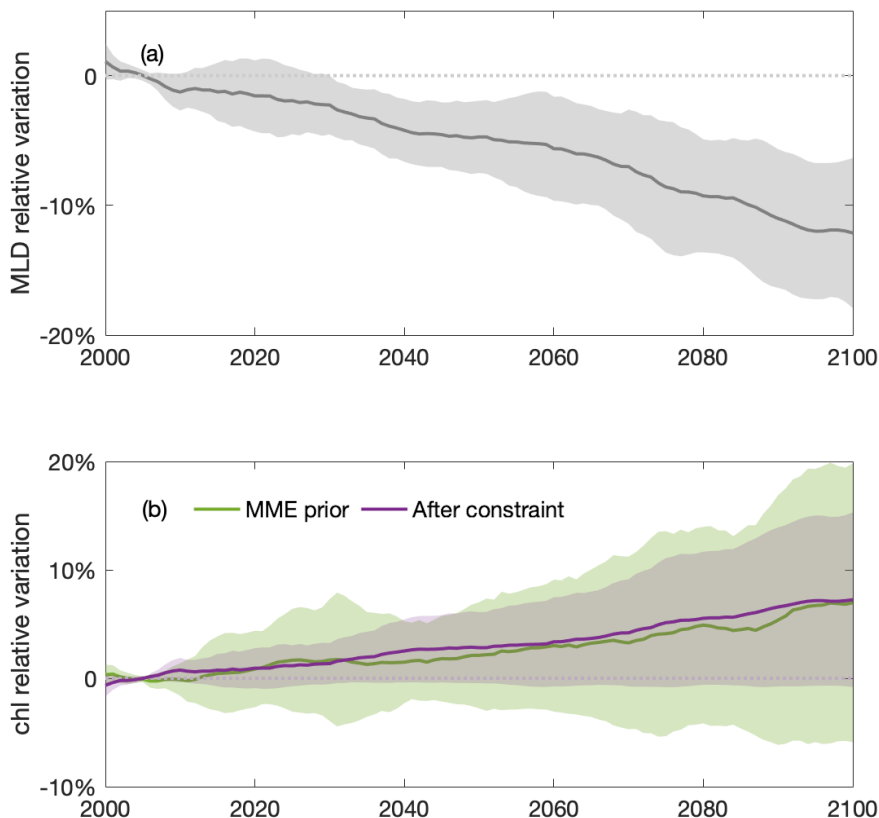


**Figure 6.** Shoaling of annual mean mixed layer depth (MLD) and increasing annual mean surface chlorophyll (chl), a proxy for surface phytoplankton biomass, towards the end of the century in the Southern Ocean. Multi-model ensemble (MME) projections of changes of annual mean (a) MLD (grey); and (b) surface chl concentration before (light green) and after (purple) applying emergent constraint, from 2000 - 2100, relative to the mean values of the first decade of the 21<sup>st</sup> century (2000 - 2009), with shading indicating one standard deviation, under the SSP5-8.5 scenario. The time series are filtered using a 10-year moving average.

such as the Southern Ocean) with a shoaling MLD, the shoaling also increases top-down grazing pressure for phytoplankton under climate change due to the rising phytoplankton concentration.

Increased top-down grazing pressure results in higher trophic transfer efficiency (Eq. 5, Fig. 8b) and integrated zooplankton biomass (Fig. 8a). The rising trophic transfer efficiency indicates a change in trophic structure, with relatively more zooplankton and less phytoplankton in the future climate. In contrast to the projection of slightly decreasing depth-integrated phytoplankton biomass ( $-1 \pm 7\%$ ), the biomass of depth-integrated zooplankton, a phytoplankton predator, is projected to increase by  $3 (\pm 9)\%$  under climate change (Fig. 8a). Zooplankton is thus favoured by changing environmental conditions and food resources and is grazing down phytoplankton. The phenomenon of a positive change on a higher trophic level and a negative change on the

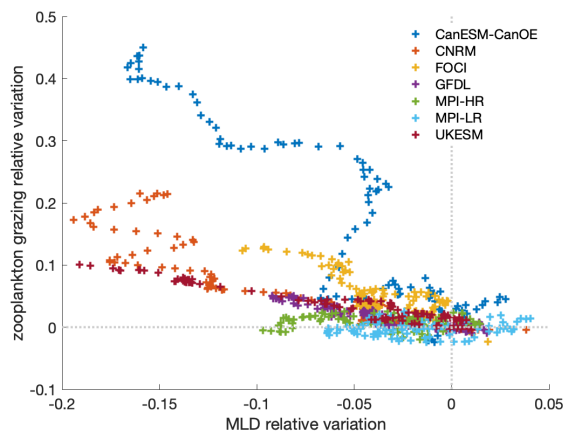


**Figure 7.** Relation between annual mean relative anomalies of mixed layer depth and zooplankton grazing from 2000 - 2100 under the SSP5-8.5 scenario, relative to the mean values of the first decade of the 21<sup>st</sup> century (2000 - 2009) in the Southern Ocean. The time series are filtered using a 10-year moving average; different colours denote different climate models.

170 lower trophic level indicates increasing top-down control of the lower trophic level by the higher one (Fig. 1 in Chust et al., 2014).

### 3.3 Constraining the increasing phytoplankton concentration: the underlying mechanism of intensified top-down control

#### 3.3.1 Opposing trends of phytoplankton concentrations and mixed layers on climate change and seasonal scales

175 Surface phytoplankton concentration is an indicator of grazing pressure and, thereby, top-down control, but its projected changes from the 2000s to the 2090s remain uncertain ( $6 \pm 12\%$ ; Fig. 6). Individual model projected changes range from -8% to +35% and in particular include zero and negative changes of surface chlorophyll in the Southern Ocean by the end of the century. Previous studies (Leung et al., 2015; Henley et al., 2020) suggested that the mechanisms behind these uncertain long-term phytoplankton changes are also the mechanisms that are responsible for seasonal phytoplankton variability in the Southern Ocean.

180 Under the current climate, seasonalities of mixed layer depths and surface chlorophyll concentration are anti-correlated in both observations and model simulations. The observed surface chlorophyll in the Southern Ocean exhibits a clear seasonal cycle, peaking in late austral spring and early austral summer (Fig. 9). This seasonal cycle of chlorophyll is opposite that of mixed layer depth (MLD), with shallow MLD in austral summer coinciding with relatively high surface chlorophyll, and deep MLD in austral winter coinciding with relatively low surface chlorophyll. Such an opposite relationship between surface chlorophyll and MLD on a seasonal scale has been previously shown in observations (Uchida et al., 2019; Arteaga et al., 2020) and model simulations (Song et al., 2018; Arteaga et al., 2020; Le Quéré et al., 2016) to be mainly caused by seasonal

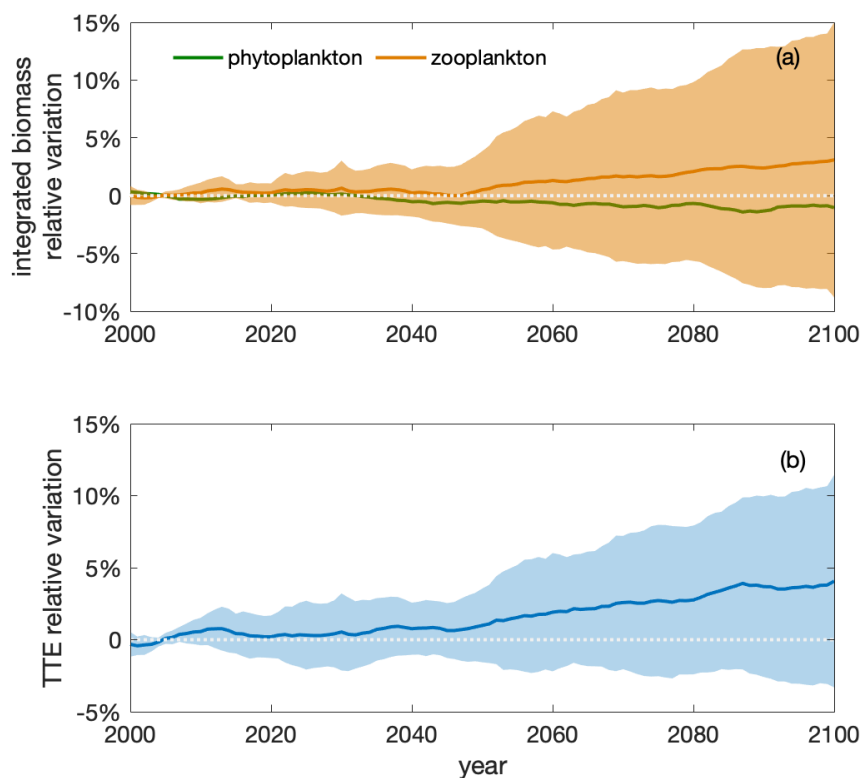


**Figure 8.** An increase in integrated zooplankton biomass and trophic transfer efficiency (TTE) during the 21<sup>st</sup> century indicates intensified top-down control and a shift in trophic structure. Multi-model ensemble (MME) projections of the relative changes of (a) depth-integrated phytoplankton (green) and zooplankton (orange) biomasses; and (b) trophic transfer efficiency (blue; see Eq. S3) from 2000 - 2100 under the SSP5-8.5 scenario, with shading indicating one standard deviation, relative to the respective mean values of the first decade of the 21<sup>st</sup> century (2000 - 2009) in the Southern Ocean. The time series are filtered using a 10-year moving average.

dilution of phytoplankton and by growth limitation along with zooplankton grazing. The individual models largely agree with the observations, though with some spread (Fig. 9). Such spread is not unexpected given the structural differences of the biogeochemical models that include varying considerations and representations of the chl:C ratio, grazing, and nutrient limitations (such as iron). Also, the modelled MLD maximum shows a lag of around a month compared to observational estimates, which is reflected in a similar lag in the chlorophyll seasonality. Additionally, there is a lag between the timing of the peaks of minimum chlorophyll and maximum MLD in winter in both observations and the models. This lag is due to poor light conditions in deep MLDs triggering an increase in the chlorophyll to carbon (chl:C) ratio, where increasing chlorophyll pigments mask a continued decrease in phytoplankton biomass (organic carbon) concentration in deepening MLDs (Geider, 1987; Arteaga et al., 2016).

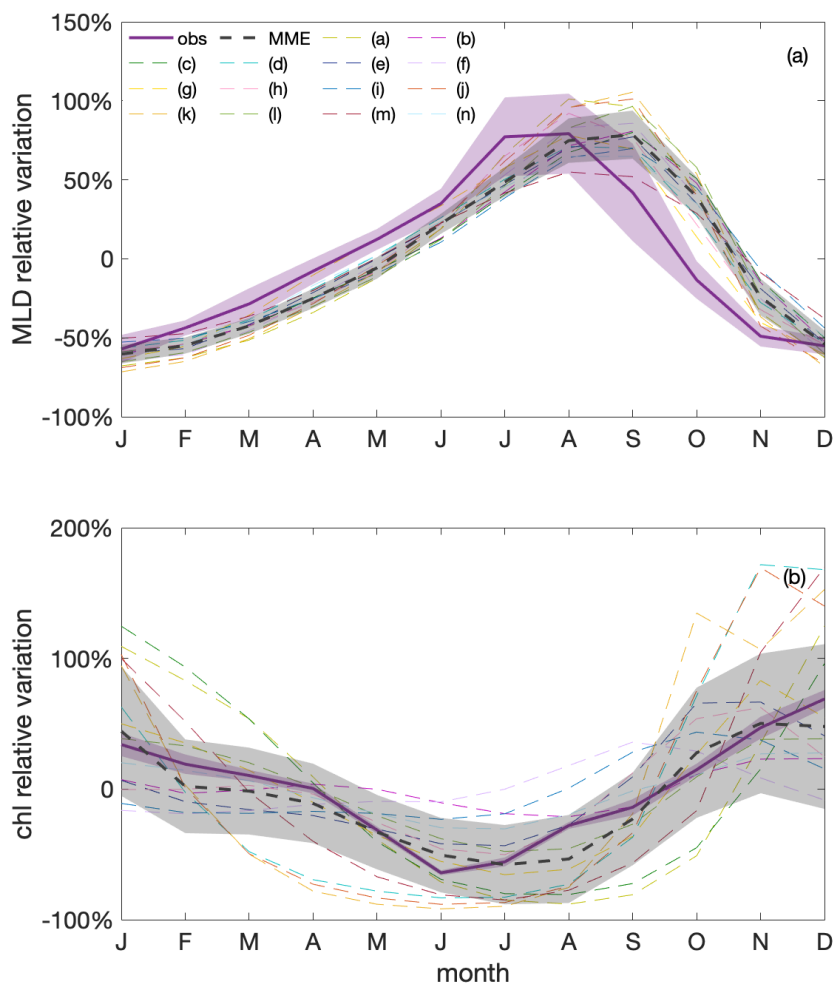


**Figure 9. Surface chlorophyll (chl) concentration shows a clear seasonal cycle that is anticorrelated with mixed layer depths (MLD) in both observations and model simulations.** Seasonal cycles of (a) MLD and (b) chl variations relative to their respective annual mean values, based on observations (GlobColour, purple) and a multi-model ensemble (MME, grey); the black dashed line marks the MME median value, and the shadings indicate the standard deviations of observations and MME, respectively. Differently coloured thin dashed lines show individual models listed in Tab. 1 that contribute to the MME median value.



### 3.3.2 Using contemporary seasonality to constrain projections of surface chlorophyll concentration

As expected based on previous studies (Leung et al., 2015; Henley et al., 2020), a linear relationship ( $r^2=0.56$ , Fig. 10a) exist across the ESM ensemble between this sensitivity of chlorophyll to changes in MLD on a seasonal scale in the current climate (seasonal sensitivity,  $S_{seas}$ , Eq. 1) and the sensitivity of chlorophyll to changes in MLD with climate change (climate change sensitivity,  $S_{clm}$ , Eq. 2). The relationship suggests that models within which surface chlorophyll is more sensitive to MLD changes on a seasonal scale also tend to show a larger sensitivity on a longer-term scale. Moreover, the slope of the emergent relationship is nearly one. A one-to-one relationship indicates the same sensitivities of the leading mechanism on different timescales (Williamson et al., 2021). The correlation between mixed layer depth and surface chlorophyll on a long-term climate scale is consistent with reduced dilution and a weakening of bottom-up controls, analogous to the most important mechanisms on seasonal scales: when the MLD is shoaling and phytoplankton is being contained in a shallower surface ocean mixed layer, average light and as a result phytoplankton concentrations increase (Xue et al., 2022b). With this, we can use the relationship to constrain the projection of phytoplankton concentration under climate change.

Applying the emergent constraint derived from the observations under current seasonality confirms the increasing trend of chlorophyll concentration with higher confidence. Utilising the observational constraint on the seasonal sensitivity  $S_{seas}$ , the emergent constraint (section 2.3) shifts the estimate of the long-term sensitivity ( $S_{clm}$ ) from  $-0.53 (\pm 0.80)$  to  $-0.59 (\pm 0.60)$  (Fig. 10b). Thus, the surface chlorophyll is slightly more sensitive to MLD shoaling than the unconstrained MME results suggest. In combination with the MME projected MLD change, our emergent constraint implies a  $7 (\pm 8)\%$  (unconstrained:  $6 \pm 12\%$ ) increase in surface chlorophyll concentrations in the Southern Ocean by the end of the 21<sup>st</sup> century (Eq. 4). The emergent constraint reduces the uncertainty in the chlorophyll projection by 38% (Fig. 6b). Based on the constraint, a phytoplankton decrease is less likely (18%) than expected based on the MME alone (30%). Our results, therefore, increase the likelihood of an increase in surface chlorophyll in the subantarctic and subpolar Antarctic regions of the Southern Ocean and thus an increase in phytoplankton concentration by the end of the century. With enhanced confidence in the projection of increasing phytoplankton concentration, the likelihood of enhanced grazing pressure, thereby intensified top-down control under climate change, also increases.

## 220 4 Discussion

### 4.1 Bottom-up control of phytoplankton under climate change

The bottom-up mechanisms that can affect phytoplankton biomass and its growth have been extensively studied using observational and modelling approaches (Deppeler and Davidson, 2017; Frenger et al., 2018; Arteaga et al., 2020). It is widely appreciated that in the subantarctic and subpolar Antarctic regions of the Southern Ocean, light limitation driven by mixed layer depth (MLD) is a primary factor that determines the seasonality of phytoplankton growth. Under climate change, phytoplankton in the Southern Ocean is expected to increase due to a positive bottom-up response to improving light conditions.

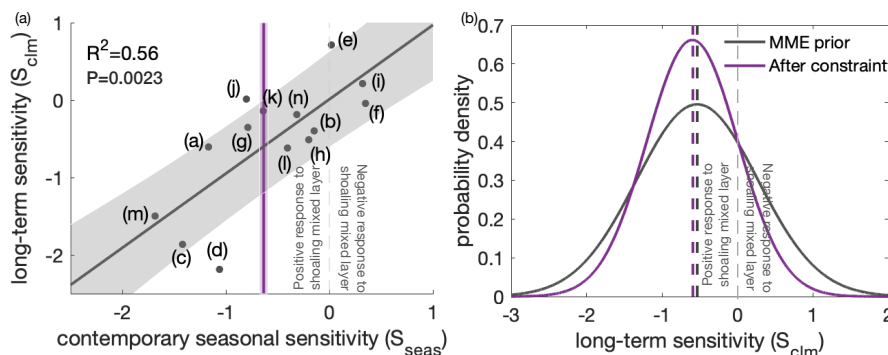


**Figure 10. Application of an emergent constraint to the long-term sensitivity of surface chlorophyll to mixed layer depth (MLD) ( $S_{clm}$ ), based on the contemporary seasonal sensitivity of chl to MLD ( $S_{seas}$ ).** (a) Long-term sensitivity ( $S_{clm}$ ) under climate change against contemporary seasonal sensitivity ( $S_{seas}$ ) of the relative variation of surface chlorophyll concentration to MLD for the multi-model ensemble (MME, black dots, corresponding to the models listed in Table. 1). The fit of a linear regression (black line) and the associated 68% prediction intervals are shown as a black line and grey shading, respectively. The purple vertical line indicates an observational constraint, with purple shading indicating the associated uncertainty, calculated as the standard error of the climatological  $S_{seas}$  of the observed time series. The light grey dashed line separates the positive (to the left) and negative (to the right) responses across models of surface chlorophyll to MLD shoaling under present-day seasonality. (b) Probability density functions (PDFs) of  $S_{clm}$ . The black line shows the "MME prior" PDF, assuming all model projections are equally likely and come from a Gaussian distribution. The purple line shows the observationally constrained PDF (it has a similar mean but is narrower). Dashed lines indicate the mean values of the future climate sensitivity before (black) and after applying the constraint (purple).

Although the increasing trend is confirmed by the simulated change in surface chlorophyll concentration, which is relatively straightforward to observe remotely, total phytoplankton in the water displays no change in the models.

In addition to light limitation, the micronutrient iron is often deemed limiting in the Southern Ocean, which would affect phytoplankton growth and limit the magnitude of phytoplankton blooms (Martin et al., 1990; Moore et al., 2013; Arteaga et al., 2020). Despite its importance to phytoplankton growth in the Southern Ocean, iron is not included in all of the models of the MME (Table 1). Over recent decades, iron stress has been observed to increase in the Southern Ocean due to changing mixed layer dynamics (Ryan-Keogh et al., 2023). However, with progressing climate change, the atmospheric iron supply, which is an important iron source for the Southern Ocean, is projected to increase through various sources (Pörtner et al., 2019; Hamilton et al., 2020). For instance, the deposition of soluble iron is expected to increase due to more frequent and intense wildfires (Bowman et al., 2020), along with increasing wind and increasing desertification (Woodward et al., 2005). As such changes in iron supply are not included in models, models with or without iron limitation do not reveal clear differences in the projection of phytoplankton response to climate change (Fig. A5).





## 4.2 Potential for top-down processes

240 While bottom-up mechanisms are well recognised, much less attention has been paid to top-down effects on phytoplankton. However, phytoplankton dynamics cannot be understood without also understanding top-down dynamics. With this study, we further look into such top-down mechanisms that drive changes in phytoplankton biomass, in particular changes in zooplankton. The formulation of zooplankton in numerical models is crucial in regulating the mortality of modelled phytoplankton, which in turn has a significant impact on planktonic dynamics (Le Quéré et al., 2016; Prowe et al., 2019). Top-down grazing by  
245 zooplankton is not only related to the total prey that is available (total phytoplankton biomass), but also to how efficiently the zooplankton can feed on the prey, which is determined, apart from traits of prey and predator, by the prey concentration (Kiørboe, 2009; Xue et al., 2022a). Our results suggest that, in addition to changing bottom-up controls, increasing top-down controls will also impact phytoplankton dynamics in the future.

Climate change projections of top-down variables are highly uncertain (Laufkötter et al., 2015; Lotze et al., 2019; Kwiatkowski  
250 et al., 2020). Despite significant advancements in ocean ecosystem monitoring and modelling abilities over recent decades, a notable gap persists in observational data and modelling efforts that specifically target zooplankton and higher trophic levels. This gap underscores the pressing need for a more comprehensive observational system, especially concerning quantities such as zooplankton biomass, community composition, and traits, to enhance the robustness of projections of future plankton dynamics and trophic transfer. The lack of adequate observational data, in particular with respect to zooplankton, has hin-  
255 dered the thorough calibration of most global biogeochemical models to properly represent top-down controls (Stock et al., 2014b). Furthermore, detailed observational research and lab experiments are also in great need. It is important to understand zooplankton physiology to identify and further constrain the relevant key parameters, such as prey preferences, maximum ingestion rates, and zooplankton temperature sensitivity (Prowe et al., 2019; Petrik et al., 2022). As far as models are concerned, both zooplankton and food web formulations in large-scale models are oversimplified, posing a substantial caveat. More easily  
260 done, zooplankton-related variables should be regularly saved as standard model output to allow for comprehensive analyses (Laufkötter et al., 2015). Additionally, not only bulk variables such as biomass but also fluxes should be saved in order to better track the energy flux through the ecosystem. Overall, model representations of phytoplankton will benefit from a more extensive assessment of zooplankton through a more accurate simulation of the top-down process.

## 4.3 Differences in trends of biomass and production

265 The divergent trends in phytoplankton biomass and production under climate change demonstrated in our study can be related to the increasing importance of top-down control. While integrated phytoplankton biomass remains relatively stable, integrated phytoplankton production continues to increase. Biomass and production represent two distinct ways of viewing and understanding the ecosystem, with one focusing on the standing stock that can be measured and the other examining the energy flow among different components of the ecosystem. A number of studies have highlighted the perspectives of biomass  
270 (Behrenfeld, 2010; Behrenfeld et al., 2017; Arteaga et al., 2020) and production (Field et al., 1998; Behrenfeld et al., 2006) to uncover the underlying mechanisms that drive the phytoplankton response under the current climate. Previous investigations



of the phytoplankton response to climate change focusing on biomass (Marinov et al., 2010; Kwiatkowski et al., 2019; Lotze et al., 2019) versus production (Behrenfeld et al., 2006; Laufkötter et al., 2015; Deppeler and Davidson, 2017; Kwiatkowski et al., 2020) tended to conclude that changes would be of the same sign for the two variables, with a negative response in low-  
275 latitude regions due to increasing nutrient limitations and a positive response in high-latitude regions as a result of improving light conditions. Further investigations into the trophodynamics using biomass (Chust et al., 2014; Kwiatkowski et al., 2019) and production (Stock et al., 2014a) have also demonstrated consistent findings, with low-latitude regions exhibiting negative trophic amplification (with decreases in higher trophic levels exceeding those in the lower trophic levels) and high-latitude regions demonstrating positive trophic amplification (with increases in higher trophic levels exceeding those in the lower trophic  
280 levels) under climate change. The change in biomass is determined by the competing effects of bottom-up (production) and top-down (loss) processes. Projections using biomass and production tend to yield the same trends when top-down processes are negligible or play a secondary role in comparison with bottom-up processes. However, it is worth noting that when top-down processes are at a level that is similar (e.g., Fig. 5) or even more important than bottom-up processes, projections using biomass and production may yield different results. Our finding of different trends in phytoplankton biomass and produc-  
285 tion underscores the increasing importance of top-down processes in the future Southern Ocean ecosystem, highlighting the differing trends in biomass and production of phytoplankton under climate change.

## 5 Conclusions

In this study, we present the future phytoplankton response to climate change under a high emission, no mitigation (SSP5-8.5) scenario in the subantarctic and subpolar Antarctic regions (40°S–60°S) of the Southern Ocean using a multi-model  
290 ensemble. We find that the depth-integrated phytoplankton biomass stays relatively stable over the course of the 21<sup>st</sup> century as a result of a dynamic balance between bottom-up and top-down control. Future phytoplankton growth conditions are expected to improve as a result of the shoaling mixed layer and, thereby, the weakening of bottom-up control, consistent with previous studies. Meanwhile, the shoaling mixed layer will further concentrate the phytoplankton biomass and make phytoplankton more accessible to zooplankton, thereby intensifying grazing pressure and hence top-down control. The continuously growing  
295 negative effect of increasing top-down control compensates for the positive effects of improving bottom-up conditions, resulting in a well-balanced flux budget that keeps the depth-integrated phytoplankton biomass stable under climate change.

We further employ the approach of an emergent constraint to increase our confidence in the increasing trend of phytoplankton concentration (using chlorophyll as a proxy), which is the underlying mechanism that contributes to the intensified top-down processes under climate change. For that, we make use of the observed relationship between seasonal variations in mixed layer  
300 depth and surface chlorophyll concentration. The relationship originates from the combined effects of bottom-up and top-down processes as well as physical dilution caused by mixing across the varying mixed layers. We use it to constrain projections of surface phytoplankton under climate change in the Southern Ocean. The application of the observational constraint to a climate projection under SSP5-8.5 scenario reduces the uncertainty of future phytoplankton projections by more than a third (from 12% to 8%). The multi-model mean projects MLD to shoal 12 ( $\pm$  5)% by the end of the 21<sup>st</sup> century, which implies, based on our



305 emergent constraint, a  $7 (\pm 8)\%$  increase in Southern Ocean surface phytoplankton concentration. Our confirmed increasing trend of phytoplankton concentration further promotes confidence in future intensified top-down control, which is driven by rising phytoplankton concentrations due to shoaling mixed layers that facilitate more efficient zooplankton feeding.

This study highlights the need to understand the balance of bottom-up versus top-down control of phytoplankton. In particular, mechanisms promoting a dominance of top-down control, which are of growing importance for climate change, have  
310 been understudied. Top-down control is typically treated stepmotherly as a mere "closure term" in biogeochemical models, serving numerical stability while typically neglecting zooplankton physiology and adaptive capacities. We argue that these are relevant to the simulation of phytoplankton. To improve our understanding of the response of phytoplankton to climate change, we need dedicated observational and modelling efforts. Such efforts include, but are not limited to, long-term and continuous observational time series of phytoplankton and zooplankton biomass and traits to enhance our understanding of the response of  
315 feeding processes to changing environmental conditions. Such observations, in turn, will facilitate improved top-down formulations in models. Further, our results suggest that previous studies (e.g., Chust et al., 2014; Kwiatkowski et al., 2017; Stock et al., 2014a) that result in the same conclusion for phytoplankton biomass and production imply a negligible or secondary role of top-down processes. With the increasing importance of top-down processes under climate change, phytoplankton biomass and production could display divergent trends, as shown in our results. Our results demonstrate that integrated phytoplankton  
320 biomass in the Southern Ocean remains stable despite increasing phytoplankton production as a result of a shifting balance from bottom-up towards enhanced top-down control.

*Author contributions.* TX and IF designed the study. TX, IF and JT conducted the analysis. All authors discussed the results and wrote the manuscript.

*Competing interests.* The authors declare that they have no conflict of interest.

325 *Acknowledgements.* This work is financially supported by the China Scholarship Council (TX, grant no.201808460055). Jens Terhaar acknowledges funding from the Woods Hole Oceanographic Institution Postdoctoral Scholar Program. We would like to thank Wolfgang Koeve and Markus Schartau for discussions and constructive feedback.



## Appendix A: Additional figures

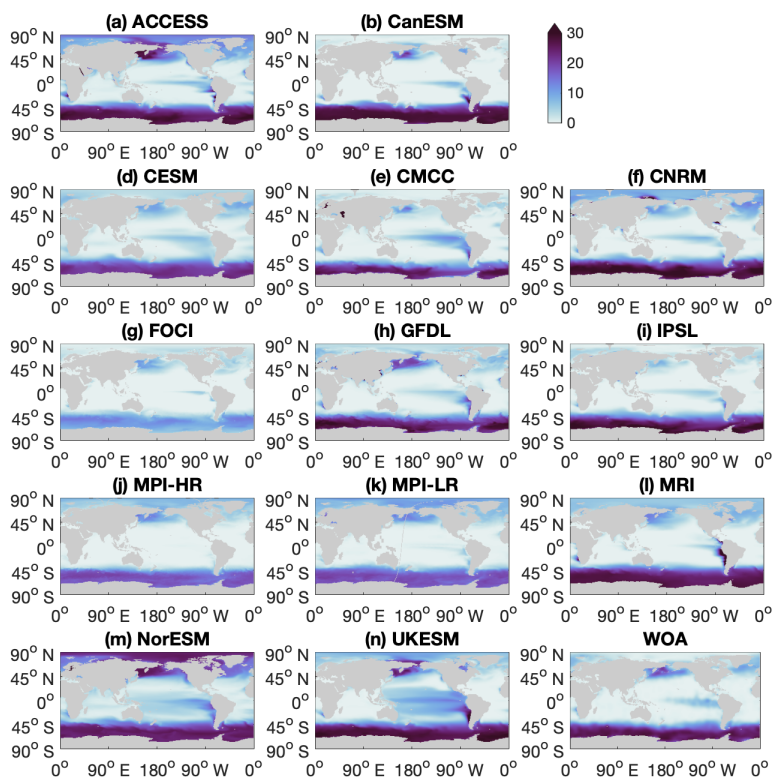


**Figure A1.** Maps for individual climate models and observational data from the World Ocean Atlas, showing annual mean surface nitrate concentration (unit:  $mmol\ m^{-3}$ ) in contemporary climate (2000s).

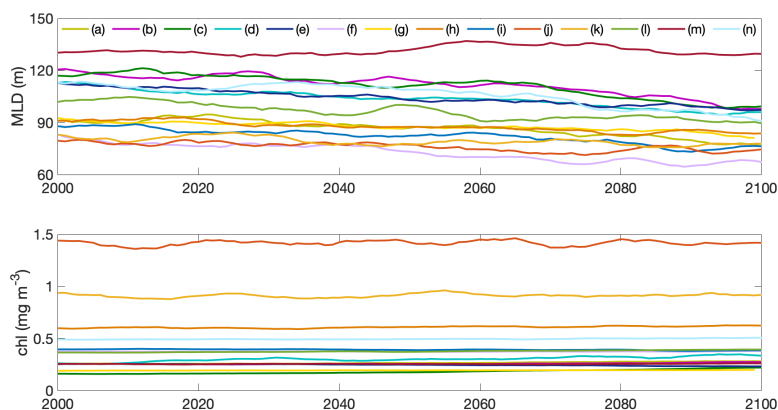


**Figure A2.** Projections of mixed layer depth (top) and surface chlorophyll concentration (bottom) in absolute values from 2000 to 2100 of individual models of the multi-model ensemble. Different coloured lines show individual models listed in Table 1 of the main manuscript.

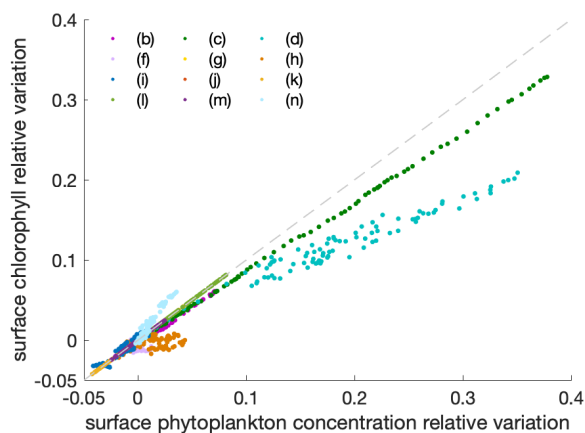


**Figure A3.** Relation between the annual mean relative variation of surface phytoplankton concentration and surface chlorophyll concentration. The light grey dashed line indicates the 1:1 line. Differently coloured dots indicate individual models as listed in Table 1 in the main manuscript, with individual dots representing consecutive years of for the time period 2000 to 2100.

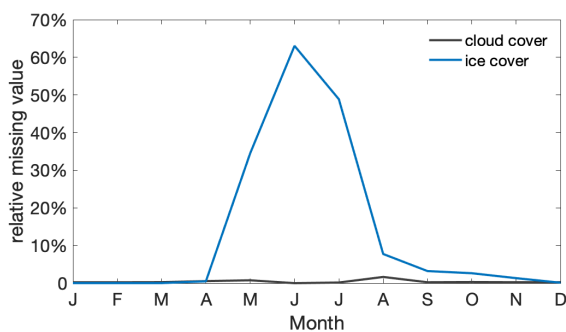


**Figure A4.** Seasonal cycle of the average portion of satellite chlorophyll missing per grid box within the research area due to cloud cover (black) and ice cover/no light (blue).

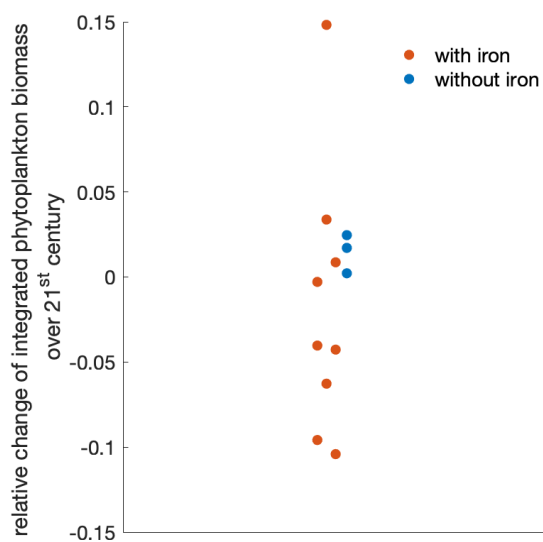


**Figure A5.** ESMs that include or do not include iron limitation project the total phytoplankton change similarly. Beeswarm plot of the relative variation of integrated phytoplankton biomass over the 21<sup>st</sup> century under the SSP5-8.5 scenario using models that explicitly include iron limitation (red) and no iron limitation (blue).



## References

- 330 Arteaga, L. A., Pahlow, M., and Oschlies, A.: Modeled Chl: C ratio and derived estimates of phytoplankton carbon biomass and its contribution to total particulate organic carbon in the global surface ocean, *Global Biogeochemical Cycles*, 30, 1791–1810, <https://doi.org/10.1002/2016GB005458>, 2016.
- Arteaga, L. A., Boss, E., Behrenfeld, M. J., Westberry, T. K., and Sarmiento, J. L.: Seasonal modulation of phytoplankton biomass in the Southern Ocean, *Nature Communications*, 11, 1–10, <https://doi.org/10.1038/s41467-020-19157-2>, 2020.
- 335 Barnes, C., Maxwell, D., Reuman, D. C., and Jennings, S.: Global patterns in predator–prey size relationships reveal size dependency of trophic transfer efficiency, *Ecology*, 91, 222–232, <https://doi.org/10.1890/08-2061.1>, 2010.
- Behrenfeld, M. J.: Abandoning Sverdrup’s critical depth hypothesis on phytoplankton blooms, *Ecology*, 91, 977–989, <https://doi.org/10.1890/09-1207.1>, 2010.
- Behrenfeld, M. J., O’Malley, R. T., Siegel, D. A., McClain, C. R., Sarmiento, J. L., Feldman, G. C., Milligan, A. J., Falkowski, P. G., Letelier, R. M., and Boss, E. S.: Climate-driven trends in contemporary ocean productivity, *Nature*, 444, 752–755, <https://doi.org/10.1038/nature05317>, 2006.
- 340 Behrenfeld, M. J., Hu, Y., O’Malley, R. T., Boss, E. S., Hostetler, C. A., Siegel, D. A., Sarmiento, J. L., Schullien, J., Hair, J. W., Lu, X., and Rodier, S.: Annual boom–bust cycles of polar phytoplankton biomass revealed by space-based lidar, *Nature Geoscience*, 10, 118–122, <https://doi.org/10.1038/ngeo2861>, 2017.
- 345 Bopp, L., Monfray, P., Aumont, O., Dufresne, J.-L., Le Treut, H., Madec, G., Terray, L., and Orr, J. C.: Potential impact of climate change on marine export production, *Global Biogeochemical Cycles*, 15, 81–99, <https://doi.org/10.1029/1999GB001256>, 2001.
- Bopp, L., Aumont, O., Cadule, P., Alvain, S., and Gehlen, M.: Response of diatoms distribution to global warming and potential implications: A global model study, *Geophysical Research Letters*, 32, <https://doi.org/10.1029/2005GL023653>, 2005.
- Bopp, L., Resplandy, L., Orr, J. C., Doney, S. C., Dunne, J. P., Gehlen, M., Halloran, P., Heinze, C., Ilyina, T., Seferian, R., and Vichi, M.: Multiple stressors of ocean ecosystems in the 21st century: projections with CMIP5 models, *Biogeosciences*, 10, 6225–6245, <https://doi.org/10.5194/bg-10-6225-2013>, 2013.
- 350 Bopp, L., Aumont, O., Kwiatkowski, L., Clerc, C., Dupont, L., Ethé, C., Gorgues, T., Séférian, R., and Tagliabue, A.: Diazotrophy as a key driver of the response of marine net primary productivity to climate change, *Biogeosciences*, 19, 4267–4285, <https://doi.org/10.5194/bg-19-4267-2022>, 2022.
- 355 Boucher, O., Servonnat, J., Albright, A. L., Aumont, O., Balkanski, Y., Bastrikov, V., Bekki, S., Bonnet, R., Bony, S., Bopp, L., and Vuichard, N.: Presentation and evaluation of the IPSL-CM6A-LR climate model, *Journal of Advances in Modeling Earth Systems*, 12, e2019MS002010, <https://doi.org/10.1029/2019MS002010>, 2020.
- Bowman, D. M., Kolden, C. A., Abatzoglou, J. T., Johnston, F. H., van der Werf, G. R., and Flannigan, M.: Vegetation fires in the Anthropocene, *Nature Reviews Earth & Environment*, 1, 500–515, <https://doi.org/10.1038/s43017-020-0085-3>, 2020.
- 360 Boyce, D. G., Lewis, M. R., and Worm, B.: Global phytoplankton decline over the past century, *Nature*, 466, 591–596, <https://doi.org/10.1038/nature09268>, 2010.
- Chien, C.-T., Durgadoo, J. V., Ehlert, D., Frenger, I., Keller, D. P., Koeve, W., Kriest, I., Landolfi, A., Patara, L., Wahl, S., and Oschlies, A.: FOCI-MOPS v1–integration of marine biogeochemistry within the Flexible Ocean and Climate Infrastructure version 1 (FOCI 1) Earth system model, *Geoscientific Model Development*, 15, 5987–6024, <https://doi.org/10.5194/gmd-15-5987-2022>, 2022.



- 365 Christian, J. R., Denman, K. L., Hayashida, H., Holdsworth, A. M., Lee, W. G., Riche, O. G., Shao, A. E., Steiner, N., and Swart, N. C.: Ocean biogeochemistry in the Canadian Earth system model version 5.0. 3: CanESM5 and CanESM5-CanOE, *Geoscientific Model Development*, 15, 4393, <https://doi.org/10.5194/gmd-15-4393-2022>, 2022.
- Chust, G., Allen, J. I., Bopp, L., Schrum, C., Holt, J., Tsiaras, K., Zavatarelli, M., Chifflet, M., Cannaby, H., Dadou, I., and Irigoien, X.: Biomass changes and trophic amplification of plankton in a warmer ocean, *Global Change Biology*, 20, 2124–2139, <https://doi.org/10.1111/gcb.12562>, 2014.
- 370 Danabasoglu, G., Lamarque, J.-F., Bacmeister, J., Bailey, D., DuVivier, A., Edwards, J., Emmons, L., Fasullo, J., Garcia, R., Gettelman, A., and Strand, W.: The community earth system model version 2 (CESM2), *Journal of Advances in Modeling Earth Systems*, 12, e2019MS001916, <https://doi.org/10.1029/2019MS001916>, 2020.
- Deppeler, S. L. and Davidson, A. T.: Southern Ocean phytoplankton in a changing climate, *Frontiers in Marine Science*, 4, 40, <https://doi.org/10.3389/fmars.2017.00040>, 2017.
- Dunne, J., Horowitz, L., Adcroft, A., Ginoux, P., Held, I., John, J., Krasting, J., Malyshev, S., Naik, V., Paulot, F., and Zhao, M.: The GFDL Earth System Model version 4.1 (GFDL-ESM 4.1): Overall coupled model description and simulation characteristics, *Journal of Advances in Modeling Earth Systems*, 12, e2019MS002015, <https://doi.org/10.1029/2019MS002015>, 2020.
- Field, C. B., Behrenfeld, M. J., Randerson, J. T., and Falkowski, P.: Primary production of the biosphere: integrating terrestrial and oceanic components, *Science*, 281, 237–240, <https://doi.org/10.1126/science.281.5374.237>, 1998.
- 380 Frenger, I., Münnich, M., and Gruber, N.: Imprint of Southern Ocean mesoscale eddies on chlorophyll, *Biogeosciences*, 15, 4781–4798, <https://doi.org/10.5194/bg-15-4781-2018>, 2018.
- Frölicher, T. L., Rodgers, K. B., Stock, C. A., and Cheung, W. W.: Sources of uncertainties in 21st century projections of potential ocean ecosystem stressors, *Global Biogeochemical Cycles*, 30, 1224–1243, <https://doi.org/10.1002/2015GB005338>, 2016.
- 385 Geider, R. J.: Light and temperature dependence of the carbon to chlorophyll a ratio in microalgae and cyanobacteria: implications for physiology and growth of phytoplankton, *New Phytologist*, pp. 1–34, <https://doi.org/10.1111/j.1469-8137.1987.tb04788.x>, 1987.
- Hall, A., Cox, P., Huntingford, C., and Klein, S.: Progressing emergent constraints on future climate change, *Nature Climate Change*, 9, 269–278, <https://doi.org/10.1038/s41558-019-0436-6>, 2019.
- Hamilton, D. S., Moore, J. K., Arneeth, A., Bond, T. C., Carslaw, K. S., Hantson, S., Ito, A., Kaplan, J. O., Lindsay, K., Nieradzick, L., and Mahowald, N. M.: Impact of changes to the atmospheric soluble iron deposition flux on ocean biogeochemical cycles in the Anthropocene, *Global Biogeochemical Cycles*, 34, e2019GB006448, <https://doi.org/10.1029/2019GB006448>, 2020.
- 390 Henley, S. F., Cavan, E. L., Fawcett, S. E., Kerr, R., Monteiro, T., Sherrell, R. M., Bowie, A. R., Boyd, P. W., Barnes, D. K., Schloss, I. R., and Shantelle, S.: Changing biogeochemistry of the Southern Ocean and its ecosystem implications, *Frontiers in Marine Science*, 7, 581, <https://doi.org/10.3389/fmars.2020.00581>, 2020.
- 395 Holte, J. and Talley, L.: A new algorithm for finding mixed layer depths with applications to Argo data and Subantarctic Mode Water formation, *Journal of Atmospheric and Oceanic Technology*, 26, 1920–1939, <https://doi.org/10.1175/2009JTECHO543.1>, 2009.
- Kessler, A. and Tjiputra, J.: The Southern Ocean as a constraint to reduce uncertainty in future ocean carbon sinks, *Earth System Dynamics*, 7, 295–312, <https://doi.org/10.5194/esd-7-295-2016>, 2016.
- Kjørboe, T.: A mechanistic approach to plankton ecology, *ASLO Web Lectures*, 1, 1–91, <https://doi.org/10.4319/lol.2009.tkiorboe.2>, 2009.
- 400 Kwiatkowski, L., Bopp, L., Aumont, O., Ciais, P., Cox, P. M., Laufkötter, C., Li, Y., and Séférian, R.: Emergent constraints on projections of declining primary production in the tropical oceans, *Nature Climate Change*, 7, 355–358, <https://doi.org/10.1038/nclimate3265>, 2017.





- Kwiatkowski, L., Aumont, O., and Bopp, L.: Consistent trophic amplification of marine biomass declines under climate change, *Global Change Biology*, 25, 218–229, <https://doi.org/10.1111/gcb.14468>, 2019.
- 405 Kwiatkowski, L., Torres, O., Bopp, L., Aumont, O., Chamberlain, M., Christian, J. R., Dunne, J. P., Gehlen, M., Ilyina, T., John, J. G., and Ziehn, T.: Twenty-first century ocean warming, acidification, deoxygenation, and upper-ocean nutrient and primary production decline from CMIP6 model projections, *Biogeosciences*, 17, 3439–3470, <https://doi.org/10.5194/bg-17-3439-2020>, 2020.
- Laufkötter, C., Vogt, M., Gruber, N., Aita-Noguchi, M., Aumont, O., Bopp, L., Buitenhuis, E., Doney, S. C., Dunne, J., Hashioka, T., and Völker, C.: Drivers and uncertainties of future global marine primary production in marine ecosystem models, *Biogeosciences*, 12, 6955–6984, <https://doi.org/10.5194/bg-12-6955-2015>, 2015.
- 410 Le Quéré, C., Buitenhuis, E. T., Moriarty, R., Alvain, S., Aumont, O., Bopp, L., Chollet, S., Enright, C., Franklin, D. J., Geider, R. J., and Valina, S. M.: Role of zooplankton dynamics for Southern Ocean phytoplankton biomass and global biogeochemical cycles, *Biogeosciences*, 13, 4111–4133, <https://doi.org/10.5194/bg-13-4111-2016>, 2016.
- Leung, S., Cabré, A., and Marinov, I.: A latitudinally banded phytoplankton response to 21st century climate change in the Southern Ocean across the CMIP5 model suite, *Biogeosciences*, 12, 5715–5734, <https://doi.org/10.5194/bg-12-5715-2015>, 2015.
- 415 Lotze, H. K., Tittensor, D. P., Bryndum-Buchholz, A., Eddy, T. D., Cheung, W. W., Galbraith, E. D., Barange, M., Barrier, N., Bianchi, D., Blanchard, J. L., and Worm, B.: Global ensemble projections reveal trophic amplification of ocean biomass declines with climate change, *Proceedings of the National Academy of Sciences*, 116, 12907–12912, <https://doi.org/10.1073/pnas.1900194116>, 2019.
- Lovato, T., Peano, D., Butenschön, M., Materia, S., Iovino, D., Scoccimarro, E., Fogli, P., Cherchi, A., Bellucci, A., Gualdi, S., and Masina, S.: CMIP6 Simulations With the CMCC Earth System Model (CMCC-ESM2), *Journal of Advances in Modeling Earth Systems*, 14, e2021MS002814, <https://doi.org/10.1029/2021MS002814>, 2022.
- 420 Marinov, I., Gnanadesikan, A., Toggweiler, J., and Sarmiento, J. L.: The Southern Ocean biogeochemical divide, *Nature*, 441, 964–967, <https://doi.org/10.1038/nature04883>, 2006.
- Marinov, I., Doney, S., and Lima, I.: Response of ocean phytoplankton community structure to climate change over the 21st century: partitioning the effects of nutrients, temperature and light, *Biogeosciences*, 7, 3941–3959, <https://doi.org/10.5194/bg-7-3941-2010>, 2010.
- 425 Martin, J. H., Gordon, R. M., and Fitzwater, S. E.: Iron in Antarctic waters, *Nature*, 345, 156–158, <https://doi.org/10.1038/345156a0>, 1990.
- Mauritsen, T., Bader, J., Becker, T., Behrens, J., Bittner, M., Brokopf, R., Brovkin, V., Claussen, M., Crueger, T., Esch, M., and Roeckner, E.: Developments in the MPI-M Earth System Model version 1.2 (MPI-ESM1.2) and its response to increasing CO<sub>2</sub>, *Journal of Advances in Modeling Earth Systems*, 11, 998–1038, <https://doi.org/10.1029/2018MS001400>, 2019.
- Mitchell, B. G., Brody, E. A., Holm-Hansen, O., McClain, C., and Bishop, J.: Light limitation of phytoplankton biomass and macronutrient 430 utilization in the Southern Ocean, *Limnology and Oceanography*, 36, 1662–1677, <https://doi.org/10.4319/lo.1991.36.8.1662>, 1991.
- Moore, C., Mills, M., Arrigo, K., Berman-Frank, I., Bopp, L., Boyd, P., Galbraith, E., Geider, R., Guieu, C., Jaccard, S., and Ulloa, O.: Processes and patterns of oceanic nutrient limitation, *Nature Geoscience*, 6, 701–710, <https://doi.org/10.1038/ngeo1765>, 2013.
- Müller, W. A., Jungclaus, J. H., Mauritsen, T., Baehr, J., Bittner, M., Budich, R., Bunzel, F., Esch, M., Ghosh, R., Haak, H., and Marotzke, J.: A Higher-resolution Version of the Max Planck Institute Earth System Model (MPI-ESM1.2-HR), *Journal of Advances in Modeling Earth Systems*, 10, 1383–1413, <https://doi.org/10.1029/2017MS001217>, 2018.
- 435 Nissen, C., Gruber, N., Münnich, M., and Vogt, M.: Southern Ocean phytoplankton community structure as a gatekeeper for global nutrient biogeochemistry, *Global Biogeochemical Cycles*, 35, e2021GB006991, <https://doi.org/10.1029/2021GB006991>, 2021.
- Pauly, D. and Christensen, V.: Primary production required to sustain global fisheries, *Nature*, 374, 255–257, <https://doi.org/10.1038/374255a0>, 1995.



- 440 Petrik, C., Luo, J., Heneghan, R., Everett, J., and Harrison, A.: Assessment and constraint of mesozooplankton in CMIP6 Earth system models, *Global Biogeochemical Cycles*, 36, e2022GB007367, <https://doi.org/10.1029/2022GB007367>, 2022.
- Pörtner, H.-O., Roberts, D. C., Masson-Delmotte, V., Zhai, P., Tignor, M., Poloczanska, E., Mintenbeck, K., Nicolai, M., Okem, A., Petzold, J., and Weyer, N.: IPCC special report on the ocean and cryosphere in a changing climate, IPCC Intergovernmental Panel on Climate Change: Geneva, Switzerland, 1, 2019.
- 445 Prowe, A. F., Visser, A. W., Andersen, K. H., Chiba, S., and Kiørboe, T.: Biogeography of zooplankton feeding strategy, *Limnology and Oceanography*, 64, 661–678, <https://doi.org/10.1002/lno.11067>, 2019.
- Ratnarajah, L., Abu-Alhaija, R., Atkinson, A., Batten, S., Bax, N. J., Bernard, K. S., Canonico, G., Cornils, A., Everett, J. D., Grigoratou, M., and Yebra, L.: Monitoring and modelling marine zooplankton in a changing climate, *Nature Communications*, 14, 564, <https://doi.org/10.1038/s41467-023-36241-5>, 2023.
- 450 Ryan-Keogh, T. J., Thomalla, S. J., Monteiro, P. M., and Tagliabue, A.: Multidecadal trend of increasing iron stress in Southern Ocean phytoplankton, *Science*, 379, 834–840, 2023.
- Sarmiento, J. L., Gruber, N., Brzezinski, M., and Dunne, J.: High-latitude controls of thermocline nutrients and low latitude biological productivity, *Nature*, 427, 56–60, <https://doi.org/10.1038/nature02127>, 2004a.
- Sarmiento, J. L., Slater, R., Barber, R., Bopp, L., Doney, S., Hirst, A., Kleypas, J., Matear, R., Mikolajewicz, U., Monfray, P., and Stouffer, R.:  
455 Response of ocean ecosystems to climate warming, *Global Biogeochemical Cycles*, 18, <https://doi.org/10.1029/2003GB002134>, 2004b.
- Séférian, R., Nabat, P., Michou, M., Saint-Martin, D., Voldoire, A., Colin, J., Decharme, B., Delire, C., Berthet, S., Chevallier, M., S., S., and Madec, G.: Evaluation of CNRM earth system model, CNRM-ESM2-1: Role of earth system processes in present-day and future climate, *Journal of Advances in Modeling Earth Systems*, 11, 4182–4227, <https://doi.org/10.1029/2019MS001791>, 2019.
- Séférian, R., Berthet, S., Yool, A., Palmieri, J., Bopp, L., Tagliabue, A., Kwiatkowski, L., Aumont, O., Christian, J., Dunne, J., and Yamamoto,  
460 A.: Tracking improvement in simulated marine biogeochemistry between CMIP5 and CMIP6, *Current Climate Change Reports*, 6, 95–119, <https://doi.org/10.1007/s40641-020-00160-0>, 2020.
- Sellar, A. A., Jones, C. G., Mulcahy, J. P., Tang, Y., Yool, A., Wiltshire, A., O’connor, F. M., Stringer, M., Hill, R., Palmieri, J., and Zerroukat, M.: UKESM1: Description and evaluation of the UK Earth System Model, *Journal of Advances in Modeling Earth Systems*, 11, 4513–4558, <https://doi.org/10.1029/2019MS001739>, 2019.
- 465 Shurin, J. B., Clasen, J. L., Greig, H. S., Kratina, P., and Thompson, P. L.: Warming shifts top-down and bottom-up control of pond food web structure and function, *Philosophical Transactions of the Royal Society B: Biological Sciences*, 367, 3008–3017, <https://doi.org/10.1098/rstb.2012.0243>, 2012.
- Song, H., Long, M. C., Gaube, P., Frenger, I., Marshall, J., and McGillicuddy Jr, D. J.: Seasonal variation in the correlation between anomalies of sea level and chlorophyll in the Antarctic Circumpolar Current, *Geophysical Research Letters*, 45, 5011–5019, 2018.
- 470 Steinacher, M., Joos, F., Frölicher, T., Bopp, L., Cadule, P., Cocco, V., Doney, S., Gehlen, M., Lindsay, K., Moore, J., and Segschneider, J.: Projected 21st century decrease in marine productivity: a multi-model analysis, *Biogeosciences*, 7, 979–1005, <https://doi.org/10.5194/bg-7-979-2010>, 2010.
- Stock, C., Dunne, J., and John, J.: Drivers of trophic amplification of ocean productivity trends in a changing climate, *Biogeosciences*, 11, 7125–7135, <https://doi.org/10.5194/bg-11-7125-2014>, 2014a.
- 475 Stock, C., Dunne, J. P., and John, J. G.: Global-scale carbon and energy flows through the marine planktonic food web: An analysis with a coupled physical–biological model, *Progress in Oceanography*, 120, 1–28, <https://doi.org/10.1016/j.pocean.2013.07.001>, 2014b.



- Swart, N. C., Cole, J. N., Kharin, V. V., Lazare, M., Scinocca, J. F., Gillett, N. P., Anstey, J., Arora, V., Christian, J. R., Hanna, S., and Winter, B.: The Canadian Earth System Model version 5 (CanESM5. 0.3), *Geoscientific Model Development*, 12, 4823–4873, <https://doi.org/10.5194/gmd-12-4823-2019>, 2019.
- 480 Tagliabue, A., Aumont, O., DeAth, R., Dunne, J. P., Dutkiewicz, S., Galbraith, E., Misumi, K., Moore, J. K., Ridgwell, A., Sherman, E., and Yool, A.: How well do global ocean biogeochemistry models simulate dissolved iron distributions?, *Global Biogeochemical Cycles*, 30, 149–174, <https://doi.org/10.1002/2015GB005289>, 2016.
- Tagliabue, A., Kwiatkowski, L., Bopp, L., Butenschön, M., Cheung, W., Lengaigne, M., and Vialard, J.: Persistent uncertainties in ocean net primary production climate change projections at regional scales raise challenges for assessing impacts on ecosystem services, *Frontiers in Climate*, p. 149, <https://doi.org/10.3389/fclim.2021.738224>, 2021.
- 485 Terhaar, J., Kwiatkowski, L., and Bopp, L.: Emergent constraint on Arctic Ocean acidification in the twenty-first century, *Nature*, 582, 379–383, <https://doi.org/10.1038/s41586-020-2360-3>, 2020.
- Terhaar, J., Frölicher, T. L., and Joos, F.: Southern Ocean anthropogenic carbon sink constrained by sea surface salinity, *Science Advances*, 7, eabd5964, <https://doi.org/10.1126/sciadv.abd5964>, 2021a.
- 490 Terhaar, J., Torres, O., Bourgeois, T., and Kwiatkowski, L.: Arctic Ocean acidification over the 21st century co-driven by anthropogenic carbon increases and freshening in the CMIP6 model ensemble, *Biogeosciences*, 18, 2221–2240, <https://doi.org/10.5194/bg-18-2221-2021>, 2021b.
- Terhaar, J., Frölicher, T. L., and Joos, F.: Observation-constrained estimates of the global ocean carbon sink from Earth system models, *Biogeosciences*, 19, 4431–4457, <https://doi.org/10.5194/bg-19-4431-2022>, 2022.
- 495 Tjiputra, J. F., Schwinger, J., Bentsen, M., Morée, A. L., Gao, S., Bethke, I., Heinze, C., Goris, N., Gupta, A., He, Y.-C., and Schulz, M.: Ocean biogeochemistry in the Norwegian Earth System Model version 2 (NorESM2), *Geoscientific Model Development*, 13, 2393–2431, <https://doi.org/10.5194/gmd-13-2393-2020>, 2020.
- Tsujino, H., Nakano, H., Sakamoto, K., Urakawa, S., Hirabara, M., Ishizaki, H., and Yamanaka, G.: Reference manual for the Meteorological Research Institute Community Ocean Model version 4 (MRI. COMv4), *Technical Reports of the Meteorological Research Institute*, 80, 306, 2017.
- 500 Uchida, T., Balwada, D., Abernathey, R., Prend, C. J., Boss, E., and Gille, S. T.: Southern Ocean phytoplankton blooms observed by biogeochemical floats, *Journal of Geophysical Research: Oceans*, 124, 7328–7343, 2019.
- Williamson, M. S., Thackeray, C. W., Cox, P. M., Hall, A., Huntingford, C., and Nijssse, F. J.: Emergent constraints on climate sensitivities, *Reviews of Modern Physics*, 93, 025 004, 2021.
- 505 Woodward, S., Roberts, D., and Betts, R.: A simulation of the effect of climate change–induced desertification on mineral dust aerosol, *Geophysical Research Letters*, 32, 2005.
- Xue, T., Frenger, I., Oschlies, A., Stock, C. A., Koeve, W., John, J. G., and Prowe, A. E.: Mixed layer depth promotes trophic amplification on a seasonal scale, *Geophysical Research Letters*, 49, e2022GL098 720, <https://doi.org/10.1029/2022GL098720>, 2022a.
- Xue, T., Frenger, I., Prowe, A., José, Y. S., and Oschlies, A.: Mixed layer depth dominates over upwelling in regulating the seasonality of ecosystem functioning in the Peruvian Upwelling System, *Biogeosciences*, 19, 455–475, <https://doi.org/10.5194/bg-19-455-2022>, 2022b.
- 510 Ziehn, T., Chamberlain, M. A., Law, R. M., Lenton, A., Bodman, R. W., Dix, M., Stevens, L., Wang, Y.-P., and Srbinovsky, J.: The Australian earth system model: ACCESS-ESM1. 5, *Journal of Southern Hemisphere Earth Systems Science*, 70, 193–214, <https://doi.org/10.1071/ES19035>, 2020.